Title

A TEMPERATURE-INDEPENDENT SPIN-LATTICE RELAXATION TIME IN METALS AT VERY LOW TEMPERATURES

Authors

Bacon, F.
Barclay, J.A.
Brewer, W.D.
et al.

Publication Date

1971-04-01

Submitted to Physical Review

UCRL-20465
Preprint

A TEMPERATURE-INDEPENDENT SPIN-LATTICE RELAXATION TIME IN METALS AT VERY LOW TEMPERATURES

F. Bacon, J. A. Barclay, W. D. Brewer
D. A. Shirley, and J. E. Templeton

April 1971

AEC Contract No. W-7405-eng-48

DISCLAIMER

A TEMPERATURE-INDEPENDENT SPIN-LATTICE RELAXATION TIME IN METALS AT VERY LOW TEMPERATURES*

F. Bacon, J. A. Barclay†, W. D. Brewer††, D. A. Shirley, and J. E. Templeton‡

Department of Chemistry and
Lawrence Radiation Laboratory
University of California
Berkeley, California 94720

April 1971

ABSTRACT

The formalism of nuclear spin-lattice relaxation at low temperatures is developed, leading to a new relaxation time T_μ and a straightforward method of interpreting very low temperature relaxation data. Data for ^{60}Co in Fe, Ni, and Co hosts and for ^{56}Co in Fe are summarized. The use of NMR in oriented nuclei for determining relaxation times is discussed, and some comments are made on the role of frequency modulation in NMR experiments with oriented nuclei.

I. INTRODUCTION

Nuclear magnetic resonance in oriented nuclei (NMR/ON), in which resonance is detected through the distribution of nuclear radiations, was suggested by Bloembergen and Temmer[1] and first observed in nuclei oriented by thermal equilibrium methods by Matthias and Holliday.[2] It was used to study relaxation in ferromagnetic metals,[3] a phenomenon that has also been studied by nonresonant methods.[4]

In 1964 Cameron et al.[5] suggested that, for nuclei relaxing in a metal through interaction with conduction electrons, the spin-lattice relaxation time T_1 will approach a constant value at temperatures low enough that the magnetic quantum γH is larger than kT. This effect was observed by Brewer et al., who reported it in abbreviated form in 1968.[6] These authors made a detailed interpretation of their relaxation data in terms of simple rate equations, finding multiexponential decay of the orientation parameters.[7,8] They found that T_1 was no longer a useful relaxation time at very low temperatures, however, and their data in ^{60}CoFe were interpreted in terms of a single exponential decay constant.

The body of this paper is divided into three parts. Section II contains a detailed discussion of the rate-equation approach to a relaxation theory for oriented nuclei, with emphasis on the physical significance of the single-exponential fit at very low temperatures. Several applications to experimental data are given in Sec. III. Section IV contains a brief discussion of the extent to which resonant destruction of nuclear orientation may be achieved through frequency modulation.

II. RELAXATION THEORY

The theory of longitudinal, or spin-lattice, relaxation of oriented nuclei is discussed in this section. The effect of relaxation on the time evolution of statistical tensors in the high-temperature limit is reviewed and its modifications for finite temperatures is considered. For nuclei in metals relaxing through $A\vec{S}\cdot\vec{I}$ interactions with conduction electrons, it is shown that the characteristic relaxation time in the low-temperature limit is temperature-independent and equal to $kC/h\nu I$, where C is the high-temperature Korringa constant ($C = T_1T$) and ν is the Larmor frequency.

The rate-equation interpretation is described below essentially as it was originally used by Brewer et al.[6-8] Two other derivations are now available. Using the Liouville-space formalism, Gabriel[9] developed a general theory of relaxation, which gives the results discussed below as a special case. More recently Hartmann-Boutron and Spanjaard[10,11] have also discussed this problem, obtaining the same results. Two other analyses of experimental measurements--in ^{60}CoCo[12] and in ^{60}CoFe and ^{60}CoNi[13]--have also been made. These later theoretical approaches[9-11] are more general than ours. They can easily treat cases entailing transverse relaxation, for example. In application to the present problem, however, only longitudinal relaxation is involved, and the three approaches give identical equations. Thus we shall retain the simpler formulation of Brewer, et al.[6-8]

A. The Question of Spin Temperature in Ferromagnetic Metals

Spin systems relax differently when a spin temperature exists than when one does not. Although both cases are treated below, it seems useful to discuss first whether spin temperatures are expected in NMR/ON experiments.

Moriya's theoretical work[14] on relaxation in ferromagnetic metals showed that the relation $T_1 = T_2$ should hold, thereby precluding the existence of a spin temperature T_S, but early measurements on stable isotopes indicated $T_2 < T_1$. Therefore the first relaxation work with oriented nuclei was interpreted under the assumption that a T_S existed.[3] In 1967 Walstedt[15] reported spin-echo measurements on several stable nuclei which showed definitively that $T_2 \approx T_1$, and subsequent analyses[6-8] have all been made with no spin-temperature assumption. It has been pointed out that the observation of relaxation in oriented nuclei could provide a definitive test of the existence of a spin temperature in these systems.[16] This follows because the simultaneous measurement of the time-dependence of several statistical tensors would provide data that were extremely sensitive to deviations of substate populations from a spin-temperature distribution. Unfortunately it is experimentally difficult to set up initial conditions that are both reliably known and appropriate for testing the T_S hypothesis. The experiments to date have been done under conditions that were not conducive to such tests,[6,7,13] and the results could be fitted either with or without assuming that a spin temperature exists. While it is very unlikely that the systems studied to date by nuclear orientation can have spin temperatures, this question has not really been tested experimentally. It is also probable that spin systems that do have spin temperatures will be studied by nuclear orientation in the future. For these two reasons an expression for the time-evolution of the spin temperature is given below.

B. Transition Probabilities. Analogy with Two-Level Radiative Systems.

Let us assume that spin-lattice relaxation occurs via an interaction with the conduction electrons, of the form

$$A\vec{I}\cdot\vec{S} = AS_zI_z + \frac{A}{2}[S_+I_- + S_-I_+] \quad , \tag{1}$$

and that first-order perturbation theory is applicable. Here $\vec{S}$ is an effective electron-spin operator that can be related to either the orbital or spin operator of conduction electrons, or to both. The discussion below is quite general, requiring only that the nuclei relax by exchanging energy with a degenerate Fermi gas, via magnetic dipole transitions. If the nuclear energy levels are equally spaced by $h\nu$ and the $|m = -I\rangle$ state lies lowest, we may write for the transition probabilities between states $|m\rangle$ and $|m + 1\rangle$

$$W_{m,m+1} = B|\langle m + 1|I_+|m\rangle|^2 \int_0^\infty f(\epsilon)\,[1 - f(\epsilon - h\nu)]\,d\epsilon$$

$$W_{m+1,m} = B|\langle m|I_-|m + 1\rangle|^2 \int_0^\infty f(\epsilon)\,[1 - f(\epsilon + h\nu)]\,d\epsilon \quad . \tag{2}$$

Here B is a constant that contains various numerical factors including the density of states at the Fermi energy, and $f(\epsilon)$ is the Fermi-Dirac distribution function,

$$f(\epsilon) = [e^{(\epsilon - \epsilon_F)/kT_L} + 1]^{-1} \quad .$$

Here L denotes the lattice. After evaluating the matrix elements and the integrals we find

$$W_{m,m+1} = Bh\nu[I(I+1) - m(m+1)]/[e^{x_L} - 1]$$

$$W_{m+1,m} = Bh\nu[I(I+1) - m(m+1)]/[1 - e^{-x_L}] \quad , \tag{3}$$

where $x_L = h\nu/kT_L$. It is easily shown, by choosing $I = 1/2$, substituting into Eq. (3), and comparing with the rate equations in the high-temperature limit, that $B = (2kC)^{-1}$, where C is the high-temperature Korringa constant ($T_1T = C$).

The appearance of the Bose-Einstein distribution function $1/[e^{x_L} - 1]$ in $W_{m,m+1}$ suggests that the above transition probabilities should possess an interesting analogy with the radiation problem. Of course this is also expected because the states $|m\rangle$ and $|m+1\rangle$ could be connected by the emission and absorption of photons. We can rewrite $W_{m+1,m}$ as follows:

$$W_{m+1,m} = (h\nu/2kC)[I(I+1) - m(m+1)[1/(e^{x_L} - 1) + 1]$$

$$= W_{m,m+1} + (h\nu/2kC)[I(I+1) - m(m+1)] \quad .$$

Thus the downward transition probability contains two parts, a temperature-dependent part which is equal to the upward probability (in analogy to stimulated emission and absorption) and a temperature-independent part, analogous to spontaneous emission. Here temperature plays a role analogous to the occupation of the radiation field in photon processes. The appearance of stimulated and spontaneous transition probabilities is in fact a general property of transitions whose quanta of excitation obey Bose statistics and are thus more likely to enter states which are already occupied. That the quanta exchanged in

magnetic relaxation obey Bose statistics is clear not only from Eq. (3) but from the fact that a relaxation process is accompanied by a conduction electron spin-flip, i.e. an "excitation" of spin 1. This is even more apparent in the case of quadrupole relaxation, in which relaxation processes are accompanied by emission or absorption of lattice phonons which clearly obey Bose statistics. At absolute zero there are no more lattice phonons to absorb but a nucleus can still relax by exciting a phonon; i.e., spontaneous emission remains.

C. Relaxation With a Spin Temperature

At high temperatures ($kT \gg$ nuclear substate level spacings) the familiar expression[3]

$$\dot{\beta} = -\frac{1}{T_1}(\beta - \beta_L) \quad ,$$

is approximately correct. Here $\beta = \frac{1}{kT_S}$ and $\beta_L = \frac{1}{kT_L}$, where T_S and T_L are the spin and lattice temperatures, respectively. At lower temperatures this relation breaks down, and it is necessary to go back to the master equation,[17]

$$\dot{\rho}_m = \sum_n (\rho_n W_{nm} - \rho_m W_{mn}) \quad . \tag{4}$$

Here ρ_m is a diagonal element of the density matrix, and W_{mn} is the transition probability from state $|m\rangle$ to state $|n\rangle$. Starting from Eq. (4), at least two papers[13,16] have quoted expressions for $\dot{\beta}$. Shirley[16] gave an equation that is not valid at very low temperatures. Spanjaard et al.[13] gave an expression that should be valid at all temperatures, but their $\dot{\beta}$ is given implicitly in several equations. A derivation leading to an explicit result in terms of measurable quantities is given below.

When a spin temperature exists, it is easy to calculate its time evolution through that of a thermodynamic property such as the internal energy, E, of the spin system. Thus for a system of N spins

$$\frac{dE}{dt} = Nh\nu \sum_{m=-I}^{I-1} [\rho_m W_{m,m+1} - \rho_{m+1} W_{m+1,m}] \quad . \tag{5}$$

After substituting from Eq. (3), using the relation $\rho_m = e^x \rho_{m+1}$ and rearranging, we have

$$\frac{dE}{dt} = \frac{N(h\nu)^2[e^{-x_L} - e^{-x}]}{2kC[1 - e^{-x_L}]} \sum_{m=-1}^{I} [I(I+1) - m(m+1)] \rho_m \quad , \tag{6}$$

where we have used the fact that the coefficient of ρ_I vanishes in order to extend the sum to m = I. Using the expressions for average values

$$Tr\rho = 1, \; Tr(m\rho) = \langle m \rangle, \; Tr(m^2\rho) = \langle m^2 \rangle \quad , \tag{7}$$

the sum may be performed, to yield

$$\frac{dE}{dt} = \frac{N(h\nu)^2[e^{-x_L} - e^{-x}]}{2kC[1 - e^{x_L}]} [I(I+1) - \langle m^2 \rangle - \langle m \rangle] \quad . \tag{8}$$

Combining Eq. (8) with

$$\frac{dE}{dx} = Nh\nu[\langle m \rangle^2 - \langle m^2 \rangle] \quad , \tag{9}$$

and using $\dot{x} = h\nu\dot{\beta}$, we have

$$\dot{\beta} = \frac{[e^{-x_L} - e^{-x}][I(I+1) - \langle m^2 \rangle - \langle m \rangle]}{2kC[1 - e^{-x_L}][\langle m \rangle^2 - \langle m^2 \rangle]} \quad . \tag{10}$$

In a system for which $h\nu$, I, and C are known, and for which a given lattice temperature exists, Eq. (10) is a useful differential equation relating the spin temperature to its time derivative. It may be solved numerically. In the high- and low-temperature limits, for $x - x_L \ll 1$, Eq. (10) goes to

$$\lim_{T_L \to \infty} \dot{\beta} = \frac{1}{T_1} (\beta_L - \beta) \quad , \tag{11a}$$

$$\lim_{T_L \to 0} \dot{\beta} = \frac{1}{T_\mu} (\beta_L - \beta) \quad , \tag{11b}$$

where $T_\mu = kC/h\nu I$, a temperature-independent relaxation constant that is discussed in part G of this section.

D. Relaxation With No Spin Temperature

For most experiments in which nuclear radiations are used to study nuclear spin-lattice relaxation, the active nuclei are present in such low concentration that they may be taken as independent. Let us again consider nuclei in a metal, subject to a relaxation interaction of the form $\frac{A}{2}[S_+I_- + S_-I_+]$ arising from conduction electrons. The time-evolution of the set of $2I + 1$ diagonal elements of the density matrix, $\{\rho_m\}$, is still given by Eqs. (2) - (4), but without a spin-temperature constraint. Rather than dealing with the $\{\rho_m\}$ themselves, it is convenient to define a new set of quantities

$\{p_m\}$ that measure the deviation of the elements ρ_m from their equilibrium values ρ_m^0,

$$p_m = \rho_m - \rho_m^0 \quad . \tag{12}$$

Since $\dot{\rho}_m = 0$ at equilibrium, Eqs. (4) and (12), may be combined to give

$$\dot{p}_m = \sum_n (p_n W_{nm} - p_m W_{mn}) \quad . \tag{13}$$

Under the $\frac{A}{2}[S_+I_- + S_-I_+]$ interaction only transitions to the states $n = m \pm 1$ are allowed. It is instructive to regard $\dot{p}_m$ and p_m as components of $(2I + 1)$-dimensional vectors with entries labeled in the order $m = I, I - 1, \ldots -I$ (or we can use the corresponding label λ which runs from zero to $2I$). Then Eq. (13) can be written

$$\dot{\vec{p}} = \overline{\overline{F}}\,\vec{p} \quad , \tag{14}$$

where $\overline{\overline{F}}$ is a "tridiagonal" matrix with nonzero elements

$$F_{mm} = W_{m,m-1} + W_{m,m+1} = -W\{I(I+1) - m(m-1)]$$

$$+ [I(I+1) - m(m+1)]\, e^{-x_L}\} \quad ,$$

$$F_{m-1,m} = W_{m,m-1} = W[I(I+1) - m(m-1)]$$

$$F_{m,m-1} = W_{m-1,m} = W\,[I(I+1) - m(m-1)]\, e^{-x_L} \quad . \tag{15}$$

Here $W = h\nu[2kC(1 - e^{-x_L})]^{-1}$. The factor e^{-x_L} in the "upward" transitions assures that detailed balance obtains at equilibrium.

The general solution of Eq. (14) has the form:

$$\vec{p}(t) = e^{-\overline{\overline{F}}t}\,\vec{p}(0) \quad . \tag{16}$$

If $\overline{\overline{F}}$ has orthonormalized eigenvectors $\vec{\eta}^{(\lambda)}$ and corresponding eigenvalues k_λ ($\lambda = 0, 1 \ldots 2I$), then the matrix $\overline{\overline{U}}$ with columns $\vec{\eta}^{(\lambda)}$ diagonalizes $\overline{\overline{F}}$:

$$\overline{\overline{U}}^{-1}\,\overline{\overline{F}}\,\overline{\overline{U}} = \overline{\overline{K}} \quad \text{where} \quad \overline{\overline{K}}_{\lambda m} = k_\lambda \delta_{\lambda m} \quad .$$

Using $\overline{\overline{U}}$ Eq. (16) can be rewritten as

$$\vec{p}(t) = \overline{\overline{U}}\, e^{-t\overline{\overline{K}}}\, \overline{\overline{U}}^{-1}\, \vec{p}(0) \quad , \tag{17}$$

or, in component form,

$$p_m(t) = \sum_\lambda \overline{\overline{U}}_{m\lambda}\, e^{-k_\lambda t} \sum_{m'} \overline{\overline{U}}^{-1}_{\lambda m'}\, p_{m'}(0) \quad . \tag{18}$$

It is instructive to discuss separately the solutions for the high- and low-temperature limits as well as those for intermediate temperatures.

E. The High-Temperature Limit

When $x_L \ll 1$, the $\overline{\overline{F}}$ matrix is symmetric about both diagonals, and is Hermitian. The eigenvector matrix $\overline{\overline{U}}$ is thus unitary. $\overline{\overline{F}}$ has the form

$$\overline{\overline{F}}_{HT} = -2W \begin{pmatrix} I & -I & & & & \\ -I & 3I-1 & 1-2I & & & \\ & 1-2I & 5I-4 & 3-3I & & \\ & & 3-3I & \ddots & & \\ & & & & 3I-1 & -I \\ & & & & -I & I \end{pmatrix} \quad . \tag{19}$$

The eigenvalues of $\overline{\overline{F}}_{HT}$ are all different. They are given by

$$k_\lambda = -W\,\lambda(\lambda + 1) \quad \text{where} \quad \lambda = 0, 1, 2, \ldots 2I \quad . \tag{20}$$

The eigenvectors have components

$$\vec{\eta}_m^{(\lambda)} = \overline{\overline{U}}_{m\lambda} = (-1)^{I+m} \, (I - m \; I \; m | \lambda \; 0) \quad , \tag{21}$$

which are closely related to the familiar statistical tensors[18]

$$\rho_0^\lambda = \sum_m (-1)^{I+m} \, (I - m \; I \; m | \lambda \; 0) \; \rho_m \quad . \tag{22}$$

In fact for $\rho_m^{(0)} = (2I + 1)^{-1}$ (equal populations at equilibrium) and using the symmetry properties of the Clebsch-Gordan coefficients, we have

$$\sum_{m'} \overline{\overline{U}}^{-1}_{\lambda m'} \, p_{m'}(0) = (1 - \delta_{\lambda 0}) \; \rho_0^\lambda(t = 0) \quad . \tag{23}$$

Combining Eqs. (18) and (23), and left-multiplying by $\overline{\overline{U}}^{-1}$, we have

$$\rho_0^{\lambda}(t) = e^{-k_\lambda t}\, \rho_0^{\lambda}(0) \quad . \tag{24}$$

These well-known results were first given, in somewhat different form, by Abragam and Pound[19] in connection with the effects of spin-lattice relaxation on the angular correlation of γ rays. Those authors found that their perturbation factor $III_{\lambda\lambda}^{00}(t)$ decayed, under an $A\vec{I}\cdot\vec{S}$ interaction, with a single exponential decay law, $e^{-k_\lambda t}$, with (in our notation)

$$k_\lambda = -\frac{2}{3}\,\tau_{CA}\left(\frac{A}{\hbar}\right)^2 I(I+1)\,S(S+1)[1-(2I+1)\,W(Il\lambda I;II)] \quad . \tag{25}$$

After substituting for the Racah coefficient $W(Il\lambda I;II)$ and accounting for conduction-electron statistics by absorbing extranuclear factors in the constant W, (Abragam and Pound dealt with single paramagnetic atoms), Eq. (25) reduces to Eq. (20).

There is nothing in the structure of $\overline{\overline{U}}$ that depends uniquely on the $A\vec{I}\cdot\vec{S}$ interaction. In fact $\overline{\overline{U}}$ will reduce a more general transition matrix $\overline{\overline{G}}_H$ to its diagonal form $\overline{\overline{G}}_H'$,

$$\overline{\overline{G}}_H' = \overline{\overline{U}}^{-1}\,\overline{\overline{G}}_H\,\overline{\overline{U}} \quad . \tag{26}$$

Of course Eqs. (18) and (24) will still hold, and the ρ_0^{λ}'s will therefore each follow single exponential decay, provided that perturbation theory is applicable. Abragam and Pound gave an explicit expression for the decay constant arising from randomly oriented, axially-symmetric quadrupole perturbations, for example. We note that for a system in which both $A\vec{I}\cdot\vec{S}$ and quadrupole relaxation was present, the transition matrices would simply add, and, from Eq. (26), so

would the decay constants. Thus the high-temperature expression for $\vec{A}\vec{I}\cdot\vec{S}$ relaxations, obtained by combining Eq. (10) with Eq. (24):

$$\rho_0^\lambda(t) = \rho_0^\lambda(0)\, e^{-W\lambda(\lambda+1)t} \quad , \tag{27}$$

which is relevant to this paper, is only one instance of a more general result.[18] A special case that is contained in Eq. (27) is the Korringa Law for $\lambda = 1$

$$\rho_0^1(t) = \rho_0^1(0)\, e^{-2Wt} = \rho_0^1(0)\, e^{-t/T_1} \quad . \tag{28}$$

This expression is applicable in conventional NMR, in which the magnetization $\vec{M}$ is studied, because $\vec{M}$ transforms as the first-rank tensor ρ_0^1.

F. Intermediate Temperatures

As the lattice temperature is lowered through the region $x_L \sim 1/I$ (not, as we shall see later, $x_L \sim 1$), the relaxation behavior changes dramatically. The matrix $\overline{\overline{F}}$ loses its symmetries about both diagonals, and takes the form

$$\overline{\overline{F}} = -2W \begin{pmatrix} I & -IQ & & & & \\ -I & IQ+2I-1 & Q-2IQ & & & \\ & 1-2I & 2IQ-Q+3I-3 & \ddots & & \\ & & \ddots & & Q-2IQ & \\ & & & 1-2I & 2IQ-Q+I & -IQ \\ & & & & -I & IQ \end{pmatrix} , \tag{29}$$

with $Q = e^{-x_L}$.

The eigenvalues are still all different, but the eigenvectors $\vec{\eta}$ are now linear combinations of the $\vec{\eta}^{(\lambda)}$ encountered above in the high-temperature case. The statistical tensors are still the parameters of interest, however, because it is they that determine the magnitudes of the observable radiation distributions, which are given by[18]

$$W(\theta,t) = \sum_{\lambda=0}^{2I} \rho_0^{\lambda}(t)\, A_{\lambda}(X_2)\, P_{\lambda}(\cos\theta) \quad . \tag{30}$$

It is still possible to solve the relaxation equations for $\rho_0^{\lambda}(t)$. From Eq. (22) $\rho_0^{0}(t) = 1$ independent of time. For $\lambda \geq 1$,

$$\rho_0^{\lambda}(t) = \sum_{\lambda'=1}^{2I} G^{00}_{\lambda'\lambda}(t)^{*}\, \rho_0^{\lambda'}(0) \quad , \tag{31}$$

where[20]

$$G^{00}_{\lambda'\lambda}(t)^{*} = \sum_{m,m',i} (-1)^{2I+m+m'} \langle I - m\ Im|\lambda\ 0\rangle\ \bar{\bar{U}}_{mi}\, e^{-k_i t}\, \bar{\bar{U}}^{-1}_{im'} \langle I - m'\ Im'|\lambda'0\rangle \quad . \tag{32}$$

Four transformations are represented in this equation, from a statistical tensor representation (λ') through the m' representation into the diagonal representation (i), then through the m representation into (λ). This equation displays clearly the way in which the statistical tensors lose their simple relationship to the eigenvectors as the temperature is lowered. As the lattice temperature approaches infinity the matrix $\bar{\bar{F}}$ becomes symmetrical, the elements $\bar{\bar{U}}_{mi}$ and $\bar{\bar{U}}^{-1}_{im'}$ become Clebsch-Gordan coefficients (Eq. (21)) and, after the orthogonality of the Clebsch-Gordan coefficients has been used twice, Eq. (32) becomes

$$G^{00}_{\lambda'\lambda}(t)^* = \delta_{\lambda i}\,\delta_{\lambda' i}\, e^{-k_i t} \quad , \tag{33}$$

which, when substituted into (31), reduces to (24). At lower temperatures the above statements no longer hold because $\overline{\overline{U}}_{mi} \neq \overline{\overline{U}}^{HT}_{mi}$. Thus $G^{00}_{\lambda'\lambda}(t)$ can be finite for $\lambda \neq \lambda'$, and $\rho^{\lambda}_{0}(t)$ shows a multi-exponential dependence upon time,

$$\rho^{\lambda}_{0}(t) = \sum_{i=0}^{2I} R_{\lambda i}\, e^{-k_i t} \quad . \tag{34}$$

The coefficients

$$R_{\lambda i} = \sum_{m,m',\lambda'} (-1)^{2I+m+m'}\, \overline{\overline{U}}_{mi}\, \overline{\overline{U}}^{-1}_{im'}\, \langle I - m\ Im | \lambda\ 0 \rangle \langle I - m'\ Im' | \lambda' 0 \rangle \rho^{\lambda'}_{0} \tag{35}$$

clearly depend on both the initial conditions and on the transformation $\overline{\overline{U}}$ that diagonalizes $\overline{\overline{F}}$. Using Eqs. (30), (34), and (35) it is possible to make a multiexponential fit to experimental relaxation data. Such an analysis has been made by Brewer, Shirley, and Templeton,[7] by Barclay and Gabriel,[12,21] and recently by Spanjaard et al.[13] Somewhat different points of view about this procedure have been taken in these studies, and it seems useful to describe one of them[7] more fully here.

There are excellent physical reasons for "the" spin-lattice relaxation time, T_1, to be regarded as a fundamental quantity in conventional NMR. The most compelling single reason is probably the fact that observable quantities relax as $\exp(-t/T_1)$, i.e., T_1 is, under usual conditions, truly a relaxation time. "Usual conditions", however, means both that the high-temperature approximation

is applicable and that only quantities which transform as first-rank tensors (i.e., the magnetization) are observed. In the intermediate-temperature range, $x_L \sim 1/I$, the first condition no longer applies, and for most nuclear orientation experiments neither condition applies. In this range T_1 as defined by[17]

$$\frac{1}{T_1} = \frac{1}{2} \frac{\sum_{nm} W_{mn}(E_m - E_n)^2}{\sum_n E_n^2} \quad , \tag{36}$$

is no longer a directly useful parameter: no observable quantity relaxes as $\exp(-t/T_1)$. For this reason Brewer, et al. abandoned T_1 in favor of an effective relaxation time T_1', which they obtained by force-fitting their data with a single exponential. Of course there is no problem in defining the parameter T_1. From Eqs. (4) and (36) we obtain

$$T_1 = \frac{2kC}{h\nu} \tanh\left(\frac{h\nu}{2kT_L}\right) \quad . \tag{37}$$

The point, however, is that T_1 is not very directly related to observables, and its use therefore might tend to obscure the real physics of the relaxation process. For example, the upward and downward transition probabilities, W_+ and W_- are grossly different, as previously pointed out. Brewer, et al. took this into account and kept the two separate, plotting $(2W_+)^{-1}$ and $(2W_-)^{-1}$ in their Fig. 1. The explicit expression for these[22] quantities are obtained from Eq. (4):

$$W_+ = \frac{h\nu e^{-x_L}}{2kC(1 - e^{-x_L})} \tag{38a}$$

$$W_- = \frac{h\nu}{2kC(1 - e^{-x_L})} = W \quad . \tag{38b}$$

Of course W_+ and W_- can still be combined to yield the parameter T_1,

$$\frac{1}{T_1} = W_+ + W_- \quad , \tag{39}$$

but it seems preferable to seek a different quantity that can serve as a more useful relaxation time. Such a quantity is discussed in the next section.

Brewer, et al. analyzed their data in two ways. First, the radiation intensity $W(\theta = 0,t)$ was followed as the nuclei relaxes to the lattice temperature after resonant excitation, and the data were fitted to the function

$$W(0,t) - W(0,eq) = [W(0,t = 0) - W(0,eq)]\, e^{-t/T_1'} \quad , \tag{40}$$

to obtain the parameter T_1', an "effective" spin-lattice relaxation time.[6] Secondly, the relaxation theory outlined in Eqs. (30) - (35) was applied to the data to make a multi-exponential fit and yield T_1.[7] This latter procedure, however, seemed less satisfactory, because it depends crucially on a knowledge of the initial conditions, and the resultant T_1 was omitted from Fig. 1 of Brewer, et al.

G. The Low-Temperature Limit: A New Fundamental Spin-Lattice Relaxation Time

Brewer, et al. obtained an unexpected result from their single-exponential analysis: T_1' approached constancy at a relatively high temperature. The "characteristic temperature" $T^{(1)}$ at which T_1 approaches constancy is, from Eq. (37)

$$T^{(1)} \sim \frac{h\nu}{2k} \quad . \tag{41}$$

For the ^{60}CoFe case, $T^{(1)} \sim 4$mK. However, the temperature at which T_1' approached constancy was about an order of magnitude higher. The reason for the faster approach of T_1' than T_1 to constancy as the temperature is lowered is a combination of two features of W_+ and W_-: namely, their inequality and their different temperature dependences.[6] All observable phenomena depend on the density-matrix elements ρ_m, whose time derivatives $\dot{\rho}_m$ vary as $(1 - e^{-x_L})^{-1}$ × (the difference between W_+ and W_-), rather than as their sum. Thus the effective relaxation rate approaches its low-temperature limit much faster than does T_1. To illustrate this let us consider the time-variation of ρ_I:

$$\dot{\rho}_I(t) = -\left[\frac{h\nu I}{kC(1 - e^{-x_L})}\right]\left[\rho_I - \rho_{I-1}e^{-x_L}\right] \quad . \tag{42}$$

Now this equation reaches its limiting form

$$\dot{\rho}_I(t) = -\frac{h\nu I}{kC}\rho_I \quad , \tag{43}$$

only at absolute zero ($x_L \to \infty$). However, for $\rho_I \approx \rho_{I-1}$, a neat cancellation of the factor $(1 - e^{-x_L})$ in Eq. (42) occurs, and the limiting form (Eq. (43)) is approximately realized for any value of x_L. By contrast, the "rate" $1/T_1$ varies as the sum of W_+ and W_- (Eq. (39)). This sum approaches constancy very slowly, and T_1 therefore seems to be a singularly inappropriate parameter in terms of which one might discuss the approach of relaxation rates to their low-temperature limiting values.

At very low temperatures $x_L \to \infty$, $Q \to 0$, and $\overline{\overline{F}}$ approaches the limiting form

$$\overline{\overline{F}}_{LT} = -\frac{h\nu}{kC} \begin{pmatrix} I & 0 & & & \\ -I & 2I-1 & 0 & & \\ & 1-2I & 3I-3 & & \\ & & & \ddots & \\ & & & & \begin{matrix} 0 & \\ I & 0 \\ -I & 0 \end{matrix} \\ & & & 1-2I & \end{pmatrix} . \quad (44)$$

The matrix $\overline{\overline{F}}_{LT}$ is singular, and thus non-diagonalizable. The roots k_λ of its characteristic equation $|\overline{\overline{F}}_{LT} - k_\lambda \overline{\overline{I}}| = 0$ may be used, however, to find the limiting values of the eigenvalues of the general transition matrix $\overline{\overline{F}}$ at low temperatures. These roots are simply the diagonal elements of $\overline{\overline{F}}_{LT}$. Thus the low-temperature limiting decay constants are, for integral I: 0 (appearing once), $I(h\nu/kC)$, $(2I-1)(h\nu/kC)$, ... $\frac{I(I+1)}{2}(h\nu/kC)$ (each appearing twice). The two smallest nonzero rate constants, having the values $h\nu I/kC$, will tend to determine the rate of change of <u>all</u> observables as the lattice temperature approaches absolute zero, provided that secular equilibrium is established. In most practical experimental situations the initial conditions will lead to secular equilibrium rather quickly, and T_1' as obtained from a single-exponential analysis will closely approach its low-temperature limiting value

$$\lim_{T \to 0} T_1' = kC/h\nu I \quad , \quad (45)$$

at a relatively high temperature. Of course it is important to know, in a given experiment, whether or not secular equilibrium has been established. This

may be done by plotting $\ln W(\theta,t)$ against t for each run, and checking for constancy in the slope. A final test is provided by inspecting the values of T_1', as obtained from least-squares analysis, to see whether they do in fact approach constancy as T decreases. We emphasize these precautions because for certain sets of initial conditions careless data analysis can lead to erroneous results. For example, in some cases T_1' obtained from a single-exponential fit can exhibit a maximum before approaching its limiting value. Alternatively a multiexponential analysis may be made to obtain the smallest nonzero eigenvalue of $\overline{\overline{F}}$. However the analysis is done, the final result is the fundamental spin-lattice relaxation time

$$T_\mu = \frac{kC}{h\nu I} = \frac{kC}{\mu H} = \lim_{T \to 0} T_1' \quad . \tag{46}$$

We shall call T_μ the magnetic spin-lattice relaxation time. In the low-temperature limit T_μ plays a role which is similar to, but more general than, that of T_1 in the high-temperature limit. The following properties of T_μ are of interest:

1. In the low-temperature limit T_μ becomes a true relaxation time for all observables. Since $\lim_{T \to 0} \dot{\rho}_{-I+1} = -(1/T_\mu)\, \rho_{-I+1}$, it follows that $\lim_{T \to 0} (\dot{\rho}_0^\lambda(t) - \rho_0^\lambda(eq)) = -1/T_\mu (\rho_0^\lambda(t) - \rho_0^\lambda(eq))$, for all tensor ranks λ. A similar relation also holds for any linear combination of statistical tensors,

$$\lim_{T \to 0} \left[\sum_\lambda A_\lambda \, (\dot{\rho}_0^\lambda - \rho_0^\lambda(eq)) \right] = -\frac{1}{T_\mu} \left[\sum_\lambda A_\lambda \, (\rho_0^\lambda(t) - \rho_0^\lambda(eq)) \right] \quad . \tag{47}$$

This result is independent of whether or not a spin temperature exists (see Eq. (11)).

2. T_μ is temperature-independent. The relation

$$T_\mu H = \text{constant} = Ck/\mu \quad , \tag{48}$$

is analogous to the Korringa relation $T_1 T = C$, but expresses the fact that the relaxation rate depends on the magnetic, rather than thermal, energy. Equation (48) should hold true both for ordinary metals and for ferromagnetics, provided that H is the net field at the nucleus.

3. T_μ contains the same information that T_1 does. It is clear that both contain the Korringa constant, C. It is perhaps less obvious that both yield the nuclear spin. In fact both do, if combined with a suitable set of auxiliary experiments.

4. Finally, the approach of T_1' to constancy occurs at a temperature that is approximately a factor of 2I higher than the temperature at which T_1 approaches constancy. This is illustrated in Fig. 1. The practical consequence is that for the range of parameters commonly encountered in nuclear orientation experiments T_1' easily reaches a saturation value, provided that I is large, while T_1 barely shows any evidence of saturation. Of course T_1' may not be equal to T_μ even after T_1' appears to have reached a saturation value.

In view of the above properties of T_1' and T_μ, we advocate analysis of very low-temperature relaxation data in terms of the relaxation time T_μ rather than the parameter T_1.

Figure 2 summarizes the rate equation approach to relaxation theory outlined in this section.

III. EXPERIMENTAL RESULTS

In this section we present the results of relaxation studies based on the observation of radiation patterns from nuclei oriented at low temperatures.

In 1966, Templeton and Shirley[3] showed that a substantial increase in the degree of NMR-disorientation of nuclei at low temperatures could be obtained by frequency-modulating the applied rf power, and that spin-lattice relaxation could be observed by switching off the frequency modulation and watching the angular distribution of emitted radiation decay back to its equilibrium value. The rf power level was maintained constant to insure a constant lattice temperature T_L during relaxation. The method is summarized in Fig. 3.

The relaxation time is obtained by fitting the decay with an appropriate function, as discussed in Sec. II. At high lattice temperatures the decay is a single exponential with a time constant which is simply related to the rank of the tensor that describes the angular distribution being observed. At low temperatures $T_L \ll h\nu I/2k$ the decay is also to good approximation a single exponential with time constant T_μ. At intermediate temperatures it is a sum of exponentials with various time constants but as explained previously the relaxation rate is controlled by the slowest rate constant after secular equilibrium is reached, and thus the last part of the decay will always be a reasonable approximation to a single exponential. The time required to reach secular equilibrium depends on the initial conditions $\rho_0^\lambda(0)$ and thus if the whole curve from $t = t_0$ onward is fitted with a single exponential, the resulting time constants T_1' will be rather sensitive to initial conditions, except at very high or very low temperatures. (Of course the full multi-exponential form, Eq. (34), may be used

to fit the decay and obtain T_1 but this procedure is also sensitive to initial conditions as may be seen from Eq. (35)). The initial conditions are, in turn, influenced by the distribution of source nuclei in the sample, the presence of impurities, lattice defects, and surface irregularities, the rf skin depth, and the rf power level and modulation. Moreover, the only knowledge of initial conditions in the sample comes from the anisotropy measurement at $t = t_0$, which is an integral measurement of averages over the whole ensemble of decaying nuclei of the above variables. Thus it is important for reliable relaxation measurements that 1) the initial conditions be kept as constant as possible throughout the experiments, and 2) that the relaxation curves be fitted with single exponential functions, the starting point for fitting being $t > t_0$ and approaching $t = t_0$ only at very low temperatures. The proper starting point for fitting can easily be found by varying the starting points and checking for consistency of the resulting T_1' values. It is our experience that fitting with a multiexponential function to find T_1 is likely to give erratic results due to the lack of accurate knowledge of initial conditions. More important, T_1 is not a relaxation time, in an operational sense, at very low temperatures.

Figure 4 shows the experimental results for ^{60}CoFe obtained by the method described above. The T_1' values are those given in Ref. 6; the T_1 values (from multiexponential fits) are previously unpublished. The large scatter in T_1 is a result of variations in initial conditions. The results may be compared with those of Spanjaard et al.,[13] who used the method of rapid eddy current heating of the sample to obtain relaxation curves.[4] From the slope of the T_1 vs $1/T$ curve one can evaluate the Korringa constant C; in Table I the value so obtained is compared with a value estimated from T_1', using $T_1' \approx T_\mu = kC/h\nu I$, and with the value given by Spanjaard, et al.[13]

Figure 5 shows similar results obtained by Bacon and Brewer[23] for ^{56}CoFe. The sources were made by the reaction ^{56}Fe(p,n)^{56}Co on thin, polycrystalline Fe foils. After irradiation the foils were annealed and mounted in the NMR/ON apparatus. The resonance, at 209.0 ± 0.2 MHz, had a width (FWHM) of 1.6 MHz and a maximum of about 55% of the anisotropy could be destroyed by frequency modulated rf power. We note that somewhat higher rf power levels are required for this experiment than for ^{60}CoFe because of the higher resonant frequency and shorter relaxation time of ^{56}CoFe. The T_1' values for ^{56}CoFe in the temperature range from $1/T = 30\ K^{-1}$ to $115\ K^{-1}$ do not reach a constant value. Instead they seem to show a maximum as described in Sec. II G. This effect results from the fitting of the entire decay curve with a single exponential function; the percentage of anisotropy destroyed at $t = t_0$ varies by more than a factor of two for the data shown in Fig. 5, being about 55% at $1/T = 30\ K^{-1}$ and only 26% at $1/T = 115\ K^{-1}$. The initial shape of the decay curves (before secular equilibrium is established) is quite sensitive to this percentage and the T_1' fits are accordingly affected. Consideration of the detailed shape of the curve shows that when the initial resonant destruction of orientation is large, a single exponential fit to the whole curve will give an erroneously large value of the time constant; this accounts for the "hump" in the T_1' values in Fig. 5. Attempts were made to obtain T_1' at lower temperatures but the low rf power levels consistent with maintaining low sample temperatures were insufficient to produce a reasonable degree of resonant destruction.

As before, the slope of the T_1 values can be used to calculate C, the result being 1.46 sec K. This value may be compared with the value obtained from the ^{60}Co measurements by using

$$\frac{C_{60}}{C_{56}} = \left(\frac{\nu_{56}}{\nu_{60}}\right)^2 \text{, i.e. } C_{56} = 1.1 \text{ or } 1.6 \text{ sec } ^\circ K$$

Our value of T_1' gives an estimate of $C_{56} \sim 1.0$ sec K.

Figure 6 shows data for ^{60}CoCo obtained by Barclay[8,12] using single crystal films of cubic Co. These data were analyzed for T_1 using Gabriel's theory, as reported in Ref. 12. An attempt was made to keep the initial conditions constant over the temperature range studied; this was feasible because of the relatively low resonance frequency of 125.1 MHz and good resonant destruction obtainable. The resulting T_1' curve becomes constant near $1/T = 100\ K^{-1}$, giving a limiting value for T_1' of 23 ± 2 sec.

Finally, we give the results for relaxation of ^{60}Co in single-crystal nickel obtained by Barclay.[8] First attempts to find the resonance in polycrystalline Ni foil failed, apparently because of excessive inhomogeneous broadening of the resonance line. Later attempts using ^{60}Co activity diffused into a Ni single crystal or ^{60}Co-Ni uniaxially electroplated onto a single crystal Cu substrate gave resonance lines at $\nu_0 = 69.08 \pm 0.05$ MHz of widths from 0.6 to 1.2 MHz FWHM. Some experiments with the plated foils showed anomalies in the magnetization curves (magnetic "hardness" and switching of the easy magnetization direction) which were probably due to differential thermal contraction of the Ni foil and the Cu substrate on cooling. Only about 15% of the anisotropy could be destroyed at tolerable rf power levels. The T_1' values obtained are shown in Fig. 7. These data show large scatter, again due to unavoidable variations in initial conditions and to fitting the whole decay

curve with a single exponential function. Assuming that T_1' is constant, we find $T_1' = 15 \pm 3$ sec.

The values of Korringa constants C and magnetic relaxation times T_1' obtained from these experiments are summarized in Table I and compared with results obtained by other workers. Examination of the last three columns of Table I shows the values of C obtained in different ways are in qualitatively good agreement. A trend is obvious: relaxation rates for ^{60}Co increase as the host lattice is changed from Fe to Co to Ni. From the resonant frequencies alone one would expect the opposite trend. However, relaxation rates depend on the density of states at the Fermi energy $N(E_F)$ as well as on frequency. Thus we conclude $N(E_F)_{Ni} > N(E_F)_{Co} > N(E_F)_{Fe}$. We also note that the values of C as obtained from the single-exponential fits are in approximate agreement with those obtained by other methods. Detailed quantitative agreement among the various values of C in Table I is not yet available. Further work is necessary to establish where the errors lie in each case.

IV. ON RESONANT DESTRUCTION OF ORIENTATION AND FREQUENCY MODULATION

In this section we address ourselves briefly to the question, "Why can the nuclear orientation not be completely destroyed?" It has been shown in a number of favorable NMR/ON cases that the orientation could be nearly destroyed (i.e., perhaps 80% destroyed), but there is always some orientation left even in the best cases. This problem has been[8,24] or will be[25] discussed elsewhere in the context of frequency-modulation phenomena. For this reason an extensive treatment would be unwarranted here: we shall simply list and comment on several problems that arise in trying to destroy nuclear orientation resonantly. Most of our remarks apply to the case of a wide, inhomogeneously-broadened resonance line must be frequency-modulated in order to observe any resonance.[3] For clarity we shall refer to this as the "resonant region", and to the homogeneous lines of which it is composed as "lines".

First, in successive sweeps through the resonant region, the effects of the radiofrequency field on individual lines will add incoherently. For any set of experimental conditions a steady state is quickly established in which orientation is re-established by relaxation to the lattice at the same rate that it is destroyed by the radiofrequency field. Numerical calculations based on an approximate model (but using a realistic set of parameters) show that only $\sim 65\%$ destruction of the orientation parameter B_2 can be expected at 0.002°K even for a favorable case in which the relaxation time is 100 sec and the radiofrequency field strength 0.1 gauss.[26]

Next, in order to be effective, the modulation frequency ν_{FM} must be neither too low[24] nor too high.[8] If ν_{FM} is too low the nuclei have time to re-orient substantially between sweeps. This result was predicted by Wilson,

and it has been observed for ^{60}CoFe and ^{60}CoNi, as shown in Fig. 8. Also apparent from this figure is a decrease in resonance destruction of anisotropy at high frequencies. This result was postulated as arising from the fact that as ν_{FM} increases the FM sideband spacing eventually exceeds the effective linewidth of the homogeneous lines. Some of these lines then fall between sidebands, where they are not excited by the radiofrequency field. To test this explanation a separate experiment with ^{60}CoFe was carried out, in which the carrier frequency was modulated by a second, audio frequency ν_{FM2} = 20 Hz, while holding ν_{FM1} constant at 5 kHz. The results are shown in Fig. 9. As expected, resonant destruction of the anisotropy increases with $\Delta\nu_2$, the bandwidth of the second modulation signal FM2. The effect is completely restored when $\Delta\nu_2$ exceeds ν_{FM1}. Restoration occurs faster at a higher H_1 amplitude since the intrinsic lines are more power-broadened in this case.

Finally, the intrinsic lines are not simply Lorentzians, but show multipole structure,[18] if even-rank statistical tensors such as B_2 are studied through γ-ray anisotropy measurements. For this reason a hard-core value of alignment exists even at the resonant frequency. One would then expect that any attempt to saturate the resonant destruction effect would result in some of the intrinsic lines exhibiting the "hard-core" response function, thereby yielding an incomplete destruction of the nuclear orientation.

FOOTNOTES AND REFERENCES

*This work was done in part under the auspices of the U. S. Atomic Energy Commission. It was also supported in part by the National Science Foundation while DAS was a Senior Postdoctoral Fellow at the Free University, Berlin.

†Present address: Department of Physics, Monash University, Clayton, Victoria, Australia.

††Present address: 1. Physikalisches Institute, Freie Universität Berlin.

‡Present address: Oxford Instrument Corp., 100 Cathedral St., Annapolis, Maryland 21401.

1. N. Bloembergen and G. M. Temmer, Phys. Rev. 89, 883 (1953).
2. E. Matthias and R. J. Holliday, Phys. Rev. Letters 17, 897 (1966).
3. J. E. Templeton and D. A. Shirley, Phys. Rev. Letters 18, 240 (1967).
4. See e.g. N. J. Stone, "A Review of Recent Developments in Low Temperature Nuclear Orientation", Proc. Int'l. Conf. on Hyperfine Interactions Detected by Nuclear Radiations, Rehovoth-Jerusalem, Israel, September 6-11, 1970 (to be published).
5. J. A. Cameron, I. A. Campbell, J. P. Compton, and R. A. G. Lines, Phys. Letters 10, 24 (1964).
6. W. D. Brewer, D. A. Shirley, and J. E. Templeton, Phys. Letters 27A, 81 (1968).
7. W. D. Brewer, D. A. Shirley, and J. E. Templeton, unpublished results, 1967. This approach was partially described in Ref. 8, pages 21-29.
8. J. A. Barclay, Lawrence Radiation Laboratory Report UCRL-18986 (September 1969).
9. H. Gabriel, Phys. Rev. 181, 506 (1969).
10. F. Hartmann-Boutron and D. Spanjaard, Compt. Rend. Acad. Sci. 268B, 1260 (1969).

11. D. Spanjaard and F. Hartman-Boutron, Solid State Communications 8, 323 (1970).

12. J. A. Barclay and H. Gabriel, J. Low Temp. Phys. 4, 459 (1971).

13. D. Spanjaard, R. A. Fox, I. R. Williams, and N. J. Stone, in "Proc. Int'l. Conf. on Hyperfine Interactions Detected by Nuclear Radiations", Rehovoth-Jerusalem, Israel, September 6-11, 1970 (to be published).

14. T. Moriya, J. Phys. Soc. Japan 19, 681 (1964).

15. R. E. Walstedt, Phys. Rev. Letters 19, 146 (1967); 19, 816(E) (1967).

16. D. A. Shirley, in "Hyperfine Interactions and Nuclear Radiations", edited by E. Matthias and D. A. Shirley (North-Holland, 1968), pages 843-858.

17. C. P. Slichter, "Principles of Magnetic Resonance" (Harper and Row, 1963), pages 118-121.

18. E. Matthias, B. Olsen, D. A. Shirley, R. M. Steffen, and J. E. Templeton, "The Theory of Nuclear Magnetic Resonance Detected by Nuclear Radiations", Lawrence Radiation Laboratory Report UCRL-18413, submitted to Physical Review.

19. A. Abragam and R. V. Pound, Phys. Rev. 92, 943 (1953).

20. This is a special case, for $q = q' = 0$, of Eq. (16) in Ref. 18. The complex conjugate notation is introduced there for consistency with earlier work.

21. Reference 8, pages 81-87.

22. In Ref. 6, the symbols W_+ and W_- in the figure, which are referred to here, are different from those in their Eq. (2), which are our $W_{m,m+1}$. The signs in the matrix elements in their Eq. (2) should all be inverted.

23. F. Bacon and W. D. Brewer, 1968 (unpublished).

24. G. V. H. Wilson, Phys. Rev. 177, 629 (1969).

25. J. A. Barclay, C. G. Don, and G. V. H. Wilson, to be published.

26. Reference 8, pages 35-43, and Fig. 10.

Table I

Case	ν_0(MHz)	T_1'(sec)[a]	C from T_1'(deg-sec)[c]	C from slope (deg-sec)[d]	C(other work) (deg-sec)	Reference
^{60}CoFe	165.7(2)	67(5)[b]	2.5	1.76(10)	2.6(2)	13
^{56}CoFe	209.0(2)	∿ 25	1.0	1.46(10)	1.1 or 1.6	(e)
^{60}CoCo	125.1	23(2)	0.69	0.54(7)	0.75	(f)
^{60}CoNi	69.08(5)	15(3)	0.25	--	0.50(5)	13

[a] Average of low-temperature values in saturation range.

[b] Errors in last digit given parenthetically.

[c] Using $C \cong h\nu I\, T_1'/k$, which approaches being exact as $T_1' \to T_\mu$.

[d] As $1/T \to 0$, $T_1 T \to C$. Errors given are random only.

[e] Calculated from $C_{56} = (\nu_{60}/\nu_{56})^2 C_{60}$.

[f] Ref. 8, page 78. The value 0.75 was obtained from NMR data on stable ^{59}Co, using $C_{60} = (\nu_{59}/\nu_{60})^2 C_{59}$.

FIGURE CAPTIONS

Fig. 1. Comparison of relaxation time T_1 and T_1'. Diagram (a) at left represents relative rates of transitions between levels, showing "bottleneck" effect of slower rates between topmost and bottommost pairs of levels, which leads to an effective relaxation time close to T_μ at relatively high temperatures. Diagram (b) at right shows temperature behavior of T_1 and T_1', illustrating the saturation of the latter at a relatively high-temperature $T^{(\mu)}$. By similar triangles one sees that $\frac{T^{(\mu)}}{T^{(1)}} = 2I$.

Fig. 2. Block diagram outlining rate-equation relaxation theory and showing relationship of Korringa's Law to general theory.

Fig. 3. Illustration of T_1 measurement using NMR/ON with frequency modulation. The counting rate along the polarization axis is denoted as W(0). Subscripts denote the values of W(0) when the nuclei are in thermal equilibrium with the lattice ($W(0)_L$), in a partially disoriented steady state ($W(0)_{SS}$), or randomly oriented ($W(0)_R$). At time t_i the FM is turned on, causing resonant destruction of the nuclear orientation in the inhomogeneously broadened line. At t_s the resonance is saturated, giving a steady state counting rate $W(0)_{SS}$. At t_0 the FM is turned off and the nuclear spins relax back to equilibrium with the lattice. All or part of this relaxation curve can be fitted to obtain either T_1 or T_1'.

Fig. 4. Relaxation data for ^{60}CoFe at low temperature. The multiexponential fit T_1 points, indicated by circles, are from Ref. 6; the single-exponential fit T_1' points (triangles) are from Ref. 7. The dashed curve shows the expected hyperbolic tangent dependence of T_1. The solid curve is simply an empirical curve drawn through the T_1' data.

Fig. 5. Relaxation data for ^{56}CoFe. The triangles indicate the single-exponential T_1' fit and the circles the multiexponential fit. The dashed curve shows the hyperbolic tangent dependence expected for T_1.

Fig. 6. Relaxation data for ^{60}CoCo from Ref. 12. Here the circles, triangles, and curves have the same meanings as in Figs. 4 and 5.

Fig. 7. Relaxation data for ^{60}CoNi (single crystal). Only T_1' is shown: an average value of 15 ± 3 seconds was inferred from these data.

Fig. 8. Fractional destruction of $1 - W(\theta)$, the nuclear orientation "effect", for $\theta = 0$, plotted against the modulation frequency. Filled circles represent ^{60}CoFe, open circles ^{60}CoNi. Solid curves connect points for which $T_{Ave}^{-1} = 95°K^{-1}$, and $H_1 = 5.6$ mOe; dashed curves connect points for which $T_{Ave}^{-1} = 240°K^{-1}$, and $H_1 = 1$ mOe. In both samples the carrier frequency was centered around resonance ($\nu(^{60}$CoFe) = 166.0 MHz; $\nu(^{60}$CoNi = 69.1 MHz)).

Fig. 9. Fractional destruction of $1 - W(0)$ for ^{60}CoFe, with an applied rf field of frequency 165.4 MHz, modulated to a bandwidth of 650 kHz by an applied modulation of frequency $\nu_{FM1} = 5$ kHz. The carrier frequency is also modulated at an audio frequency of 20 Hz through a variable bandwidth $\Delta\nu_2$, shown as abcissa. For the top curve H_1 (applied, peak-to-peak) = 2.8 mOe, and $1/T = 175°K^{-1}$. In the bottom curve $H_1 = 1$ mOe, $1/T = 250°K^{-1}$.

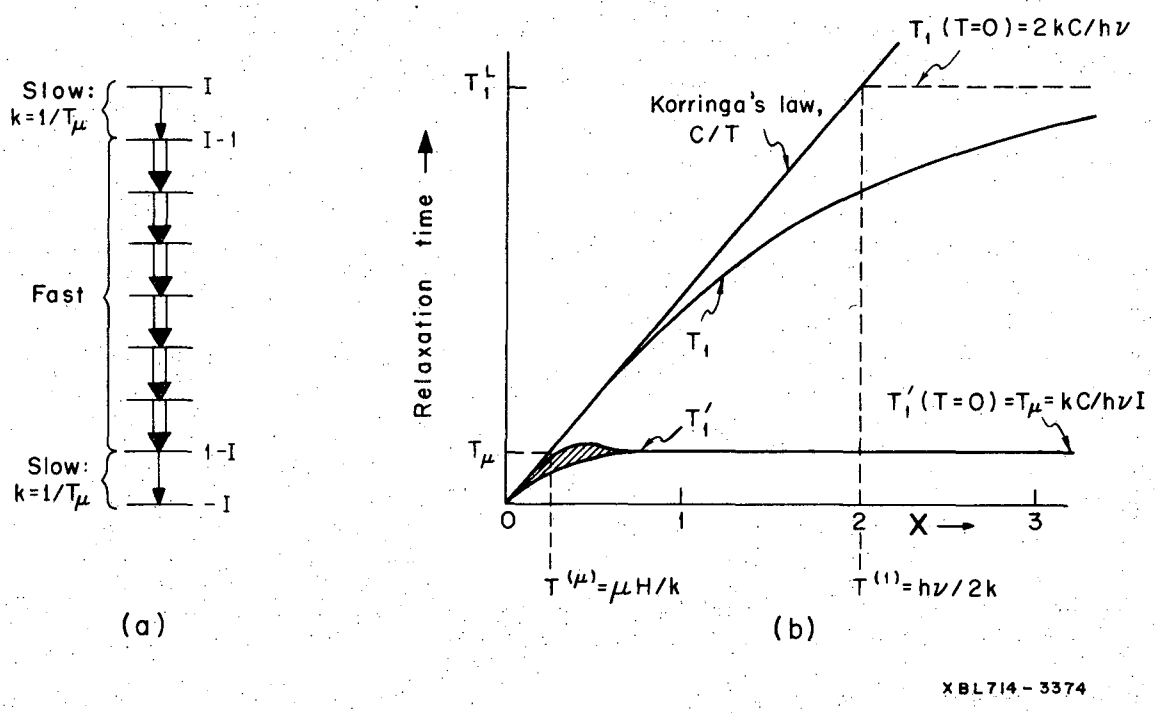
Slow:
k=1/Tμ
I
I-1
Fast
1-I
Slow:
k=1/Tμ
-I
(a)
Relaxation time
T1L
Tμ
T1 (T=0)=2kC/hν
Korringa's law,
C/T
T1
T1′
T1′(T=0)=Tμ=kC/hνI
0
1
2
X
3
T(μ)=μH/k
T(1)=hν/2k
(b)
XBL714-3374

Fig. 1

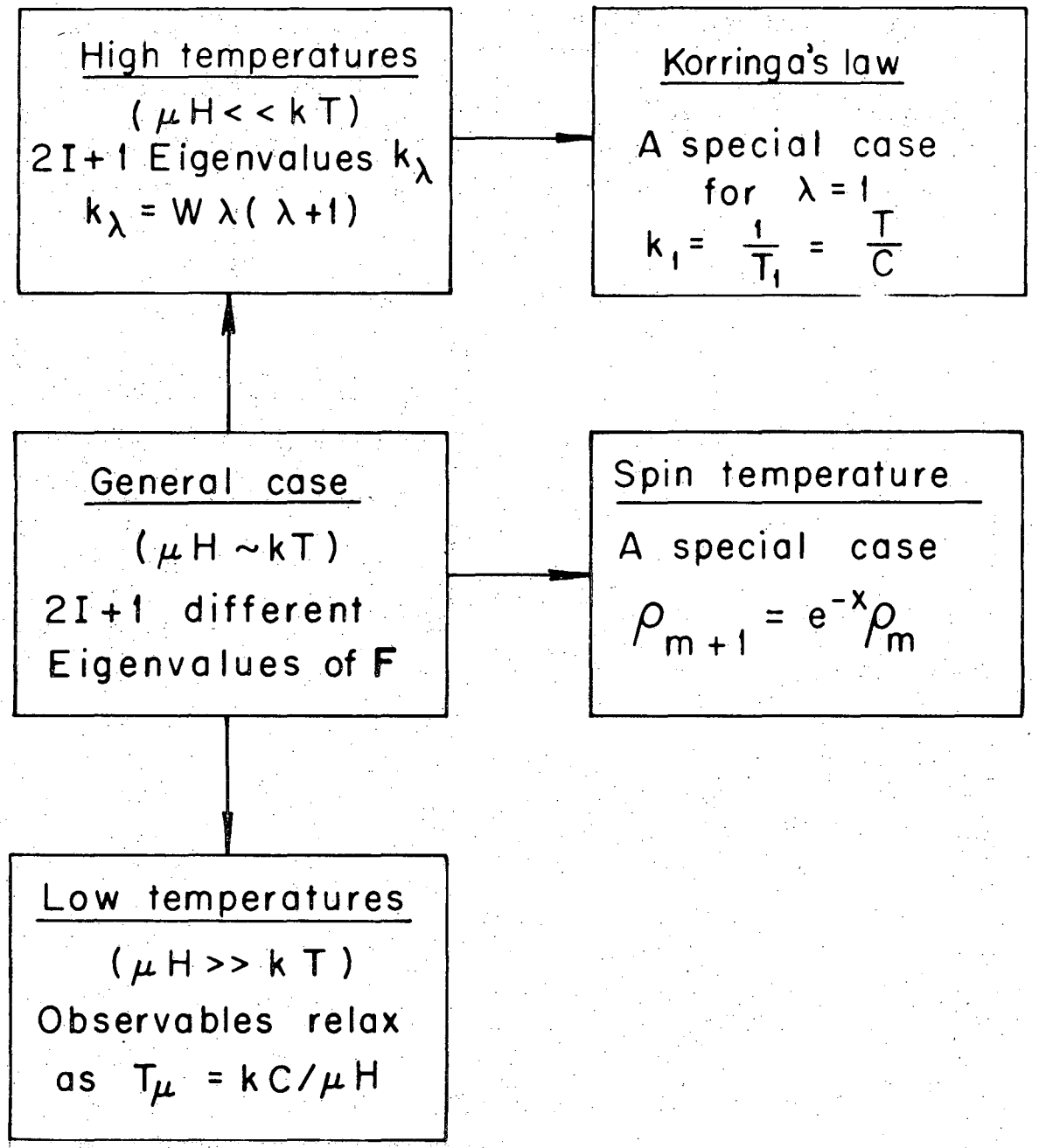
High temperatures
(μH << kT)
2I+1 Eigenvalues k_λ
$k_\lambda = W\lambda(\lambda+1)$
Korringa's law
A special case
for $\lambda = 1$
$k_1 = \frac{1}{T_1} = \frac{T}{C}$
General case
(μH ~ kT)
2I+1 different
Eigenvalues of F
Spin temperature
A special case
$\rho_{m+1} = e^{-x}\rho_m$
Low temperatures
(μH >> kT)
Observables relax
as $T_\mu = kC/\mu H$
XBL714-3373

Fig. 2

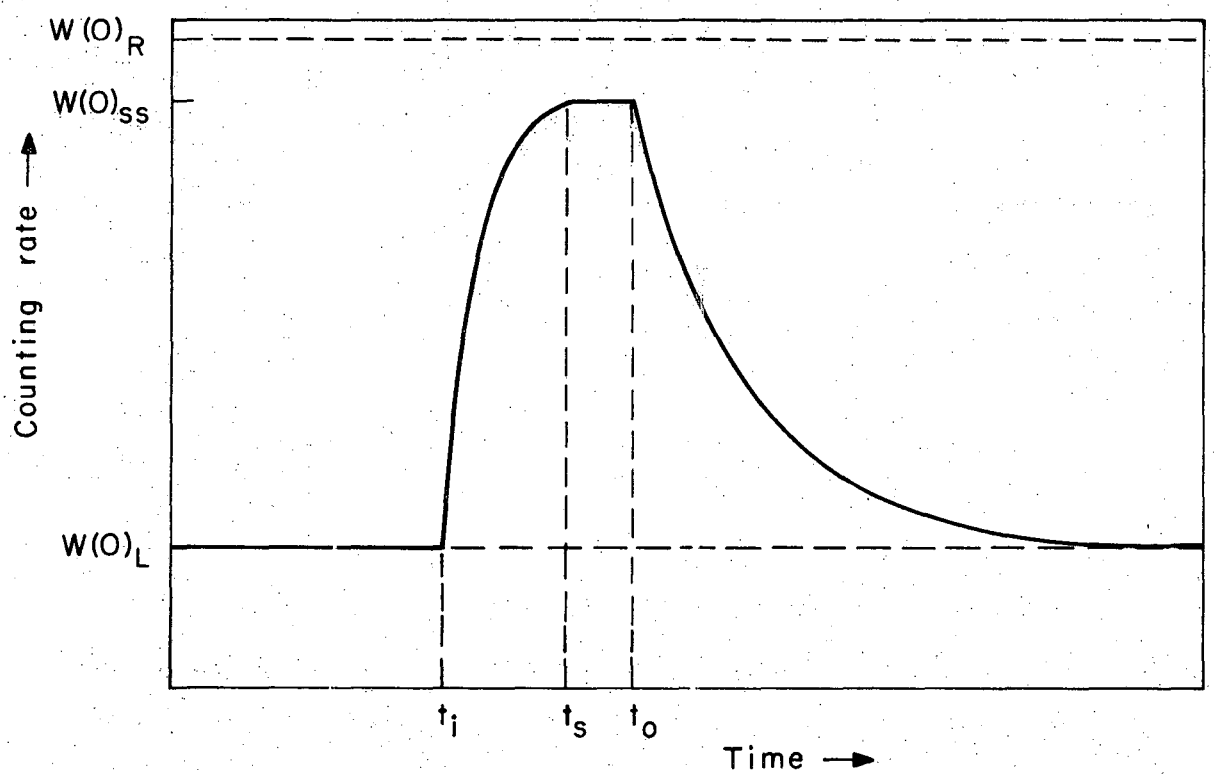

Fig. 3

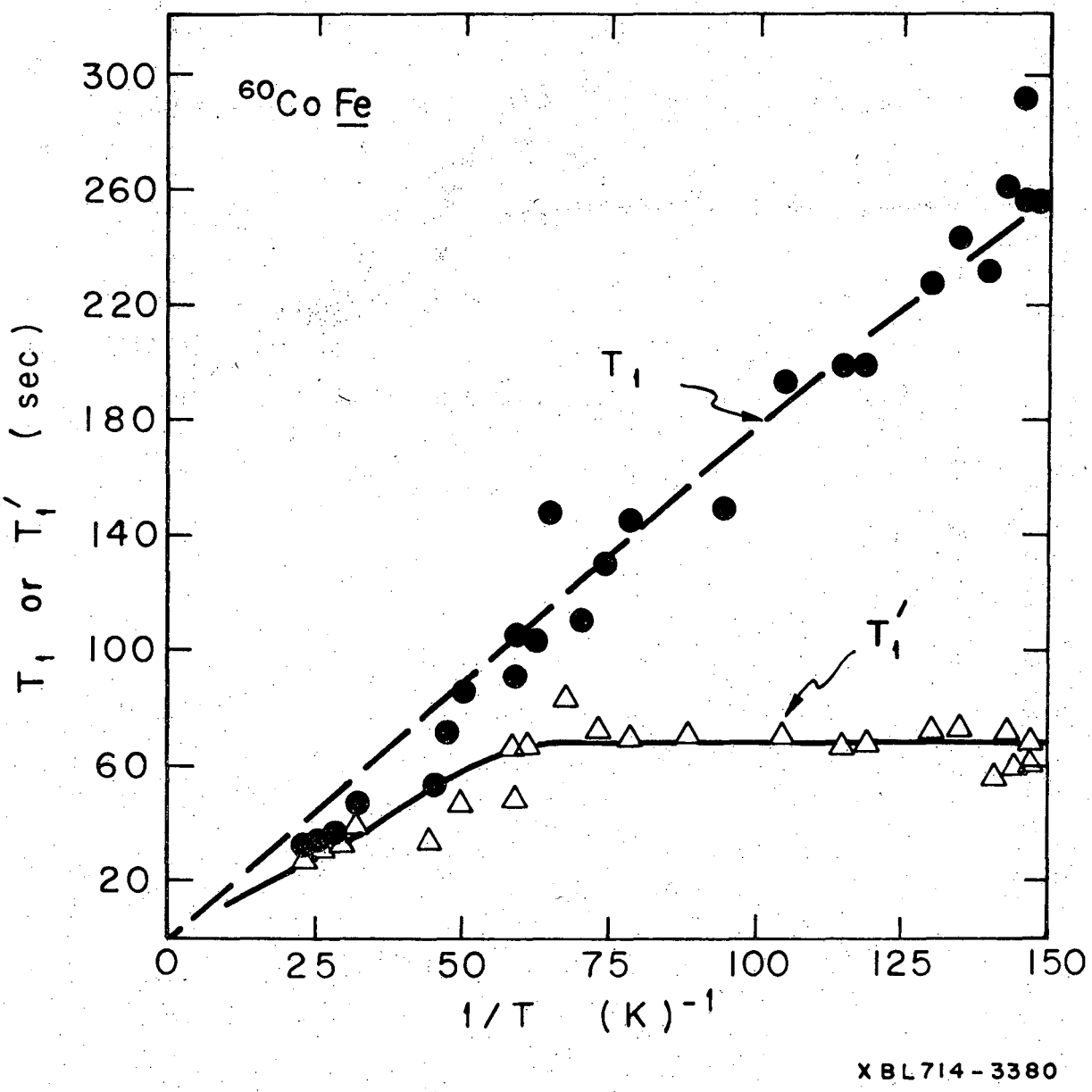
^{60}Co Fe
T_1
T_1'
T_1 or T_1' (sec)
1/T (K)$^{-1}$
300
260
220
180
140
100
60
20
0
25
50
75
100
125
150
XBL714-3380

Fig. 4

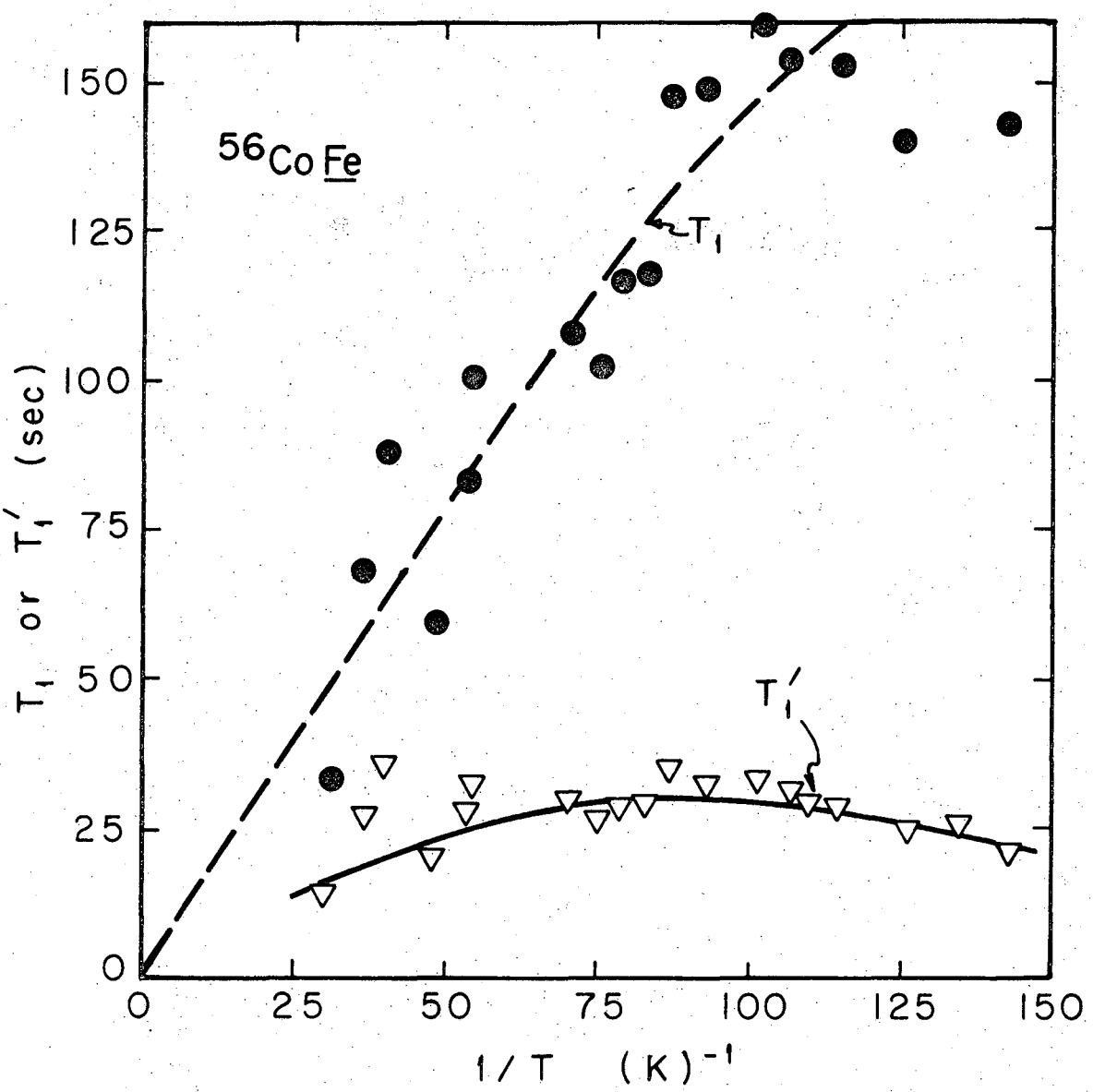

XBL714-3379

Fig. 5

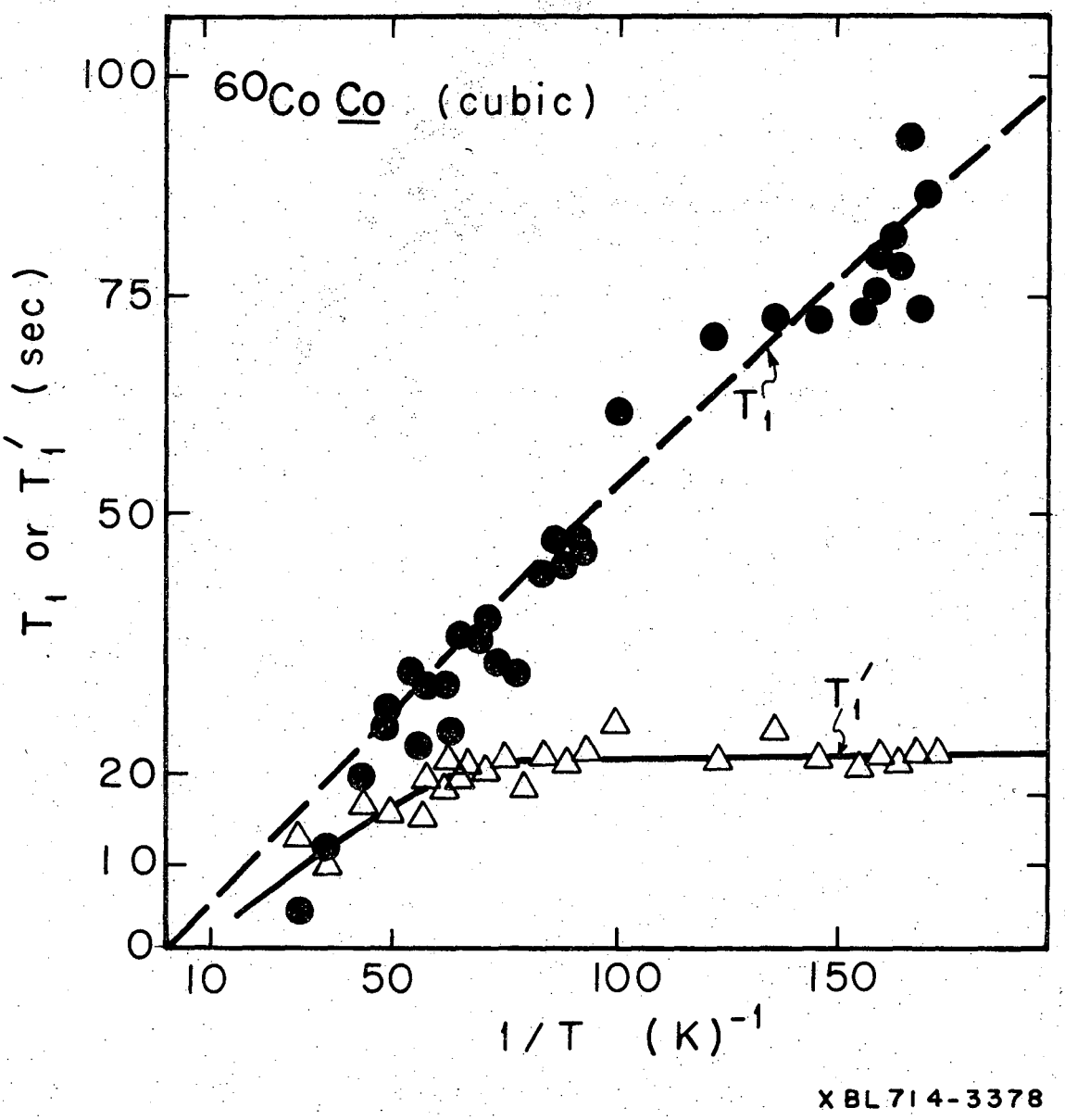
^{60}Co Co (cubic)
T_1 or T_1' (sec)
100
75
50
20
10
0
10
50
100
150
1/T (K)$^{-1}$
T_1
T_1'
XBL714-3378

Fig. 6

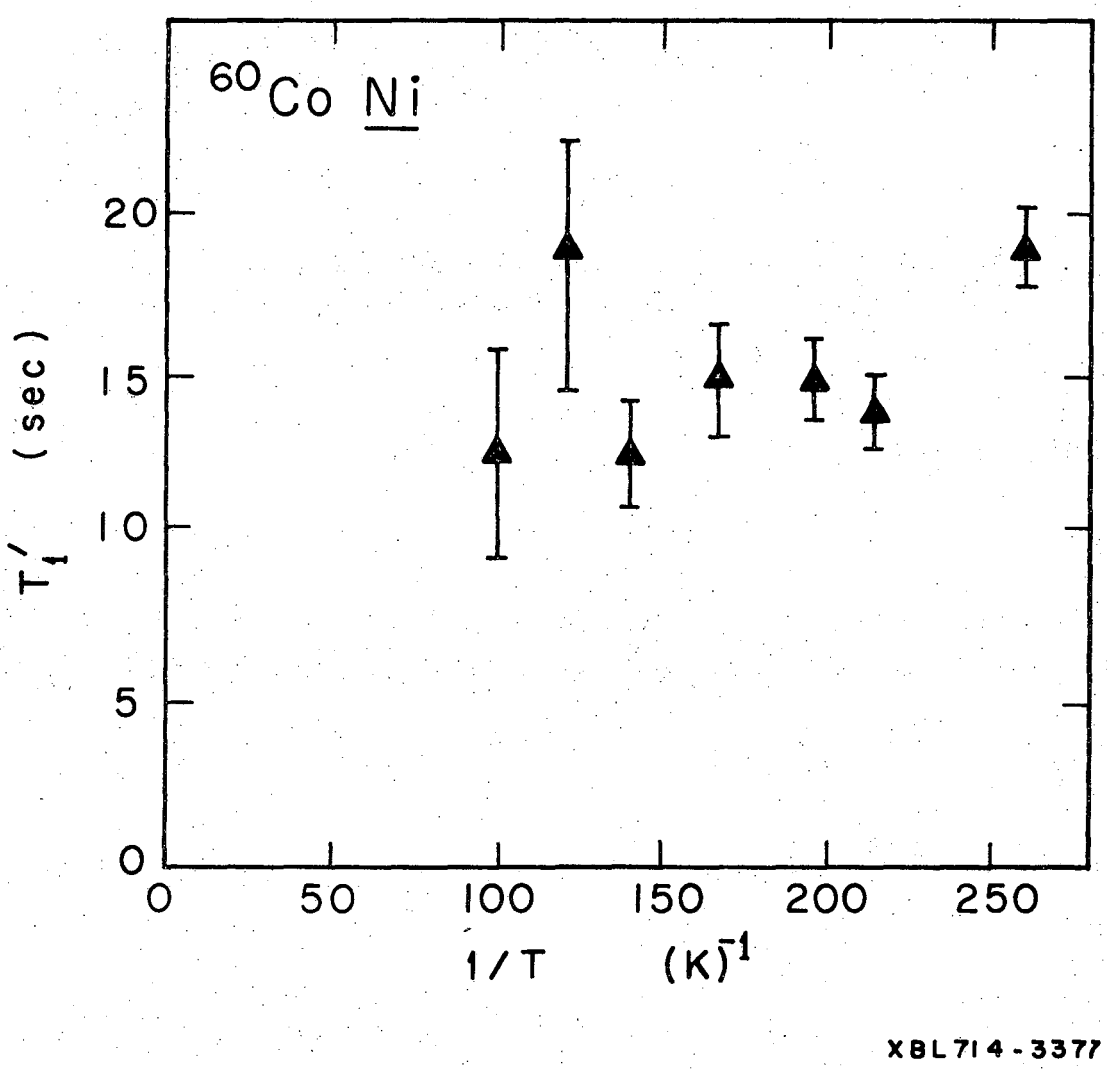

Fig. 7

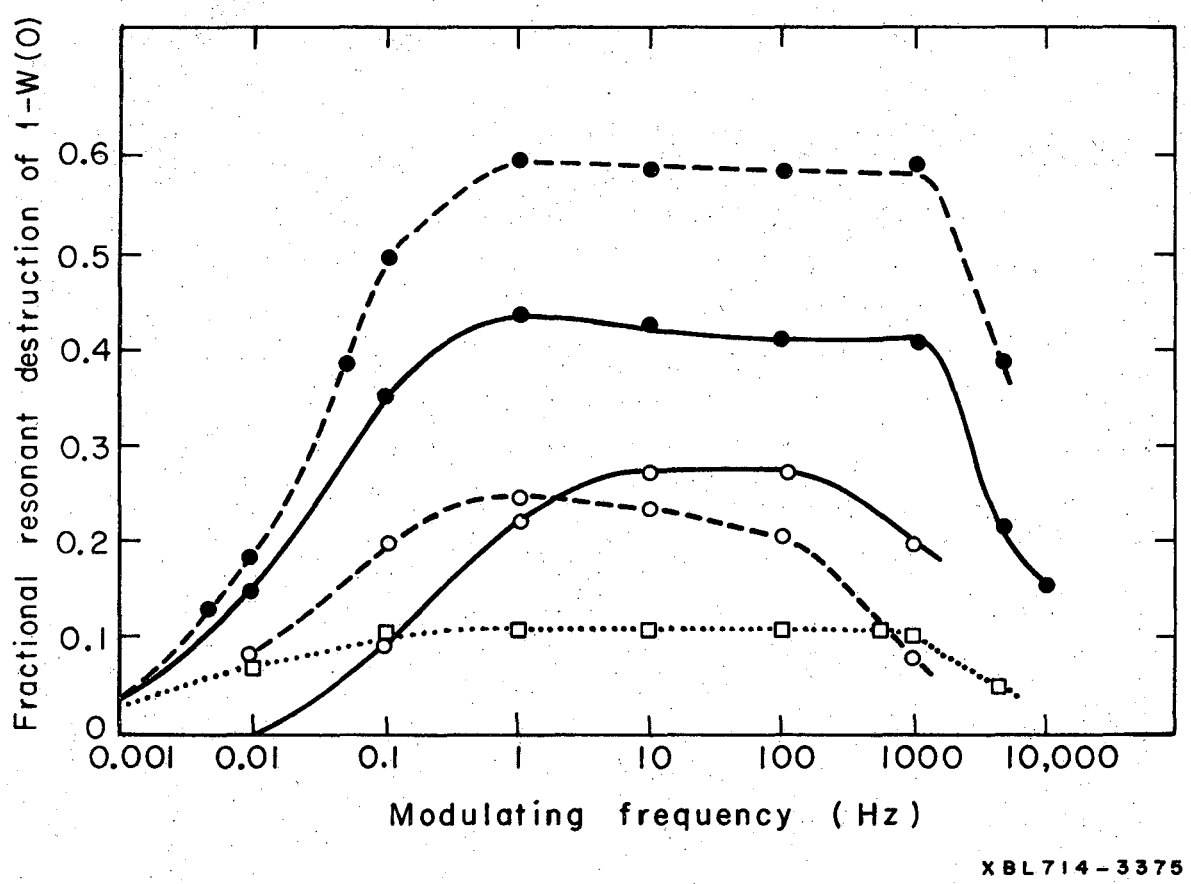
Fractional resonant destruction of 1-W(0)
0
0.1
0.2
0.3
0.4
0.5
0.6
0.001
0.01
0.1
1
10
100
1000
10,000
Modulating frequency (Hz)
XBL714-3375

Fig. 8

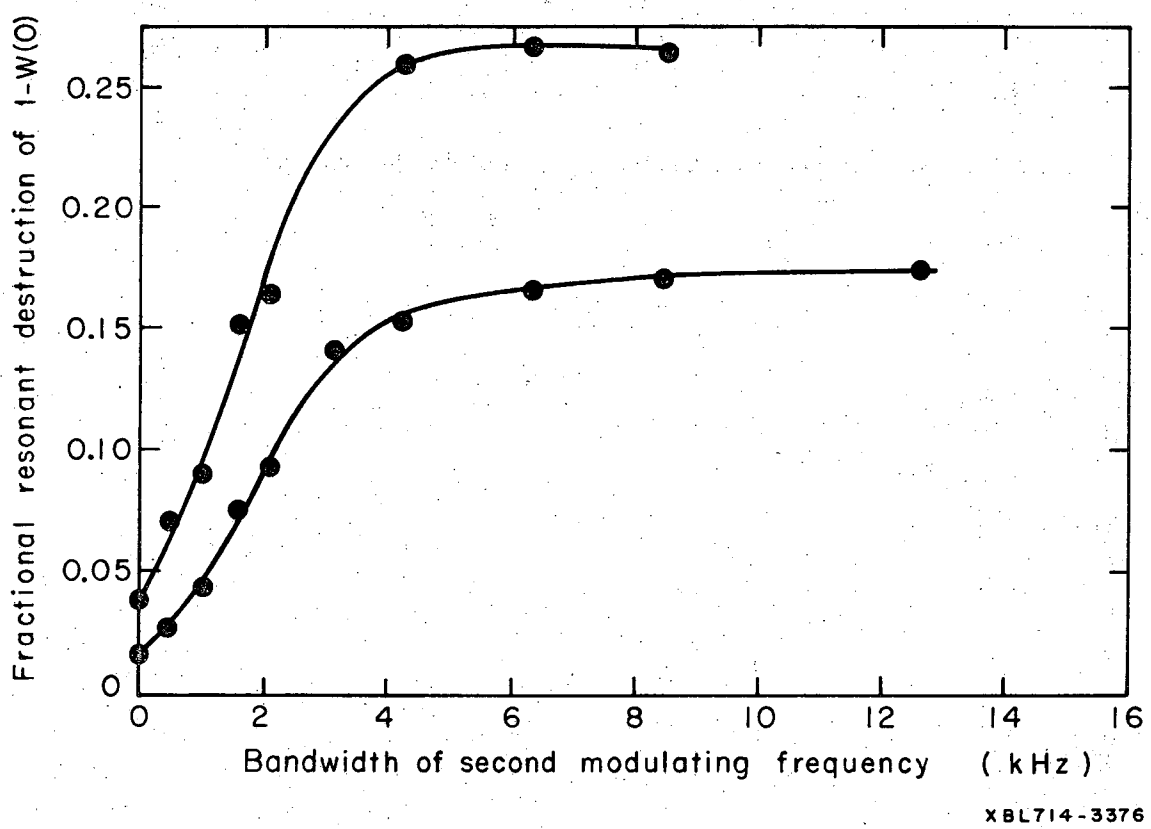
Fractional resonant destruction of 1-W(0)
0.25
0.20
0.15
0.10
0.05
0
0
2
4
6
8
10
12
14
16
Bandwidth of second modulating frequency (kHz)
XBL714-3376

Fig. 9

TECHNICAL INFORMATION DIVISION
LAWRENCE RADIATION LABORATORY
UNIVERSITY OF CALIFORNIA
BERKELEY, CALIFORNIA 94720